Preparation, Optimization, and Characterization of Biochar Using Zero Liquid Discharge (ZLD) Sludge of a Wastepaper Based Paper Mill

Kumar, Amit; Kumar Srivastava, Nirmal*+; Gera, Poonam

Department of Chemical Engineering, Dr. B. R.Ambedkar National Institute of Technology, Jalandhar-144011, Punjab, INDIA

ABSTRACT: *This paper reports the preparation of biochar from sludge generated in a wastepaper-based paper mill operating on the Zero liquid discharge principles. Biochar has been prepared from sludge, hereafter referred to as Zero liquid discharge sludge, in a laboratory muffle furnace using the slow pyrolysis method. The effect of pyrolysis temperature and pyrolysis time on biochar' yield, surface area, and pore volume of biochar has been studied by applying response surface methodology. The pyrolysis temperature and pyrolysis time were maintained in the range 450-750^{o}C and 100-200 min. respectively, under the central composite design. It was found that temperature and time significantly impacted the biochar's yield, surface area, and pore volume of biochar showing strong linear, quadratic, and interaction effects. ANOVA of the empirical models developed in this study was found to be efficient with high $R^2_{predicted}$, ($R^2_{adjusted} - R^2_{predicted}$) < 0.2, adequate precision > 4, and non-significant lack of fit value. The optimum pyrolysis temperature and pyrolysis time were determined to be 539.65°C and 176.67 min correspondingly having a desirability value 0.651. The optimized values of biochar's yield, surface area, and pore volume for Zero liquid discharge sludge biochar were found to be 63.95%, 40.23 m^2/g, and 0.048 cm^3/g respectively. The physicochemical (proximate and CHNS) and instrumental (XRD, TGA, DSC, FT-IR, and SEM) analysis along with their comparison with other biochar reported in the literature confirmed the use of this biochar as an adsorbent in wastewater treatment.*

KEYWORDS: *Pulp and paper; Sludge; Biochar; Surface area; Pore volume; Pyrolysis.*

INTRODUCTION

The contaminations of environmental resources with solid and aqueous waste generated by the chemical industries present a profound threat to the global community. Ubiquitous augmentations of these adverse organic and inorganic wastes in the environment have become a cause of serious disquiet. The important sources of these solid and aqueous pollutants are primarily anthropogenic and can be commenced into the environment by agricultural activities, mining operations, sewage activities, and products or by-products of chemical industries such as pulp and paper industries, metallurgy, electroplating, ceramics, pigment manufacturing,

** To whom correspondence should be addressed.*
+ E-mail: srivastavank@nitj.ac.in
1021-9986/2023/1/1028-1048 21/$/7.01

textile printing, plastic, and polymer industries, refined petroleum products, and detergents, etc.[1-2]. Among several chemical industries, pulp and paper mills (PPMs) discharge highly polluting wastewater and generate a myriad of solid waste [3].

Thus, realizing the environmental threats these paper mills are adopting zero liquid discharge (ZLD) concepts. The ZLD concept employs the sealing of entire process water loops by complete recycling of originated effluent, within a process cycle or into a separate process sequence across the industrial unit. Meanwhile, operating on this concept these paper mills produce a huge amount of ZLD sludge whose disposal may become another concern [4].

Paper industry sludge has been reported in the literature for the preparation of one such value-added material namely, biochar via its pyrolysis [5]. Various types of raw materials such as agricultural waste, sludge's (Sewage and industrial) have been used in making biochar to cope up with the sludge's disposal problem, wastewater treatment, and in other applications [6-8-37-42-75-76]. In wastewater treatment, ZLD sludge-based biochar can be used for the removal of typical pollutants such as heavy metals, organic pollutants, phosphorous, and nitrogen. The most common technique which is used to remove contaminants from wastewater is adsorption. Adsorption is the most versatile technique to remove contaminants from wastewater. Due to low-cost preparation, plentiful functional groups, large pore volume, high surface area, and environmental stability of biochar. Many more researchers have reported various other applications of paper industry sludge-based biochar materials [9-11]. Among various applications of biochar, biochar has emerged as a cost-effective adsorbent for wastewater treatment. Also, not much research has been done on the disposal of this paper industry ZLD sludge; preparation of biochar from ZLD sludge for wastewater treatment may be a novel attempt [12].

The physicochemical properties of biochar greatly depend on pyrolysis conditions such as temperature and residence time. Thus, an attempt has been made in this work to derive some empirical relation between pyrolysis conditions and desired properties of biochar such as yield, surface area, and pore volume [13]. This relationship was established in the process using a Response Surface Method (RSM). The RSM is primarily a florilegium of statistical and mathematical tools that use measurement data to decipher the multifactorial model equation to evaluate the physical, chemical, or biological processes with the advantages of reduced test experiments, cost, time duration, and manpower. It has also the ability to identify the presence of interactions between the factors involved in processes and to predict the responses effectively within the selected levels of factors [14].

The rest of the paper is arranged as follows. The second section describes a collection of ZLD sludge samples, preparation of ZLD sludge biochar, fundamentals of response surface methodology, and characterization techniques of ZLD sludge biochar. The third section explains the repercussions of pyrolysis temperature (Py_T) and pyrolysis time (Py_t) on biochar yield (BC_Y), surface area (BC_{SA}), and pore volume (BC_{PV}) using a derived polynomial equation. It also discusses optimum values of Py_T, Py_t, BC_Y, $BC_{SA,}$ and BC_{PV} as well as describes the characteristics of optimized biochar in terms of proximate and ultimate analysis, XRD (X-ray diffraction), TGA (thermos gravimetric analysis), DSC (differential scanning calorimetry) analysis, FT-IR (Fourier Transform Infra-Red) spectroscopy, and SEM (scanning electron microscopy). A comparative assessment of these optimized parameters concerning other biochar reported in the literature has also been carried out. Finally, the relevant conclusion has been drawn and the limitations of this study have been highlighted.

The main objective of this paper is to produce cost-effective ZLD sludge-based biochar which can be used in various purposes like soil amendment, remediation of toxic metals and organic contaminants from soil and water, and catalyst for industrial application.

EXPERIMENTAL SECTION

Materials and methods

ZLD sludge sample arrangement

ZLD sludge was arranged from a Recycled Fiber based paper mill situated in the northern part of the country. The sludge was dried for 2 weeks in the open air. Later on, after air drying, it was manually crushed to free the sludge lumps. Lump-free and air-dried ZLD sludge samples were further used for experimental analysis.

Preparation of ZLD sludge biochar

ZLD sludge was pyrolyzed using a slow pyrolysis methodology [15]. Pyrolysis is a thermal degradation

Table 1: Experimental design for biochar preparation.

Experimental event	Py_T,°C	Py_t, min	BC_{SA}, m^2/g	BC_{PV}, cc/g	BC_Y,%
1	700	120	62	0.08	48.83
2	600	192.43	38.59	0.05	63.34
3	500	180	27.78	0.04	67.12
4	741.42	150	61.17	0.06	50.02
5	600	150	54.14	0.06	56.24
6	600	150	55.94	0.06	57.71
7	600	150	57.82	0.06	55.68
8	458.58	150	19.09	0.03	69.95
9	500	120	15.62	0.03	65.17
10	600	150	59.87	0.05	56.66
11	600	150	58.93	0.06	55.50
12	700	180	37.44	0.04	54.97
13	600	107.57	49.39	0.06	52.39

of organic material in the absence of oxygen. Here slow pyrolysis is adopted rather than fast or flash pyrolysis to obtain biochar consuming less energy. Slow pyrolysis leads normally to better process control and lower emissions. Besides this, slow pyrolysis is employed to maximize the ZLD sludge-based biochar. The temperature and time maintained in the muffle furnace in between 450 to 700^0C, 100 to 200 min. A certain amount of ZLD sludge was taken in specially designed cylindrical vessels made of stainless steel. These vessels were further put in a furnace by maintaining a heating rate of 20°C/minute. The temperature and time were varied according to the central composite design stated later in the manuscript. A total of 13 sets of pyrolysis experiments were performed as per this design. The complete experimental design with 13 runs of pyrolysis temperature and time with the corresponding values of yield, surface area, and pore volume are shown in Table 1. For performing the pyrolysis experiment two input factors were taken, so depending upon the number of input factors number of experimental runs is determined. In this study, DOE selected was central composite design. According to this design, the experiment was performed at five levels, namely (–α, -1, 0, 1, +α). Here the value of α = 1.414. The slow pyrolysis of paper mill ZLD sludge according to the central composite design within the experimental range of temperature and time brought forth yield, surface area, and pore volume in the range 50.02 – 69.946%, 15.621 – 62.003 m^2/g, and 0.029 – 0.075 cm^3/g respectively. A schematic for the preparation of ZLD sludge biochar is shown in Fig. 1.

Response surface methodology

RSM was formulated by two mathematicians namely G.E.P. Box and K.B. Wilson in the year 1951. The RSM-based design of preparation, formulation of polynomial expression, analysis of results, and optimization of ZLD sludge biochar preparation was executed using Design-Expert Software version 12 (Stat-Ease, Inc.). For the preparation and optimization of ZLD sludge biochar the following strategy was adopted [16]:

- Initial design- CCD (Central composite design)
- Construction model- Quadratic polynomial
- Independent variable-Temperature (450-750°C) and time (100-200 min)
- Dependent variable (response) - Biochar yield, BET surface area, pore volume

The value was adopted to sustain flexibility and is the stretch from the center of the design domain to the star position. The numerical value of α in this study is 1.414. Test responses are included in the following polynomial model:

$$y = \omega + \sum_{i=1}^{n} \omega_i x_i + \sum_{i=1}^{n} \omega_{ij} x_i^2 + \sum_{i=1}^{n-1} \sum_{j=2}^{n} \omega_{ij} x_i x_j \quad (1)$$

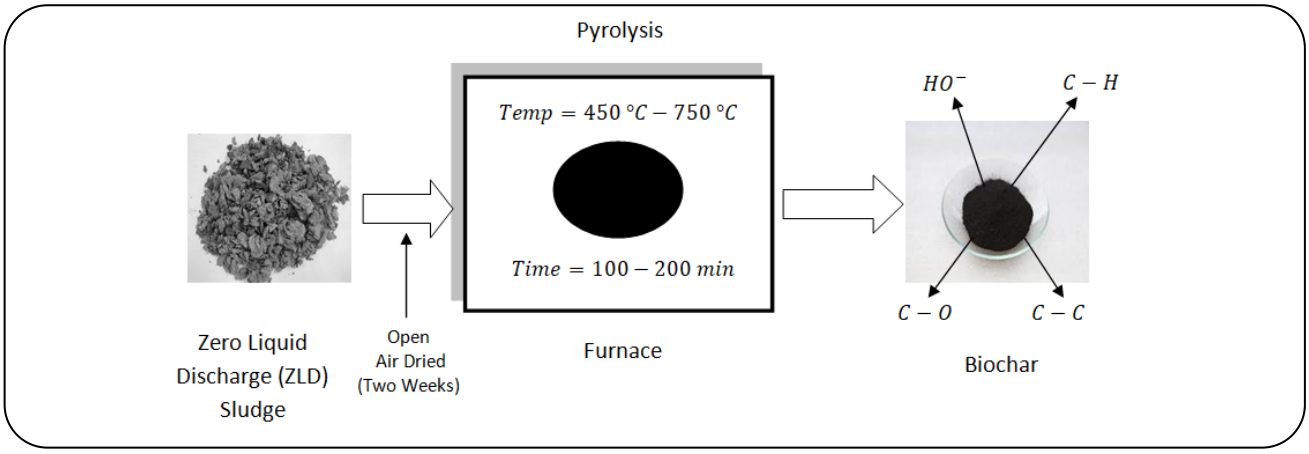

Fig. 1: Process diagram.

Here y = response, ω= the offset term, ω_i= the linear effect, ω_{ii}= the quadratic effect and ω_{ij}= interaction effect. Independent variables are indicated by x_i and x_j. The model so developed was checked for its validity using ANOVA (analysis of variance) which included verification of P-values of model, model terms and lack of fit along with $R^2_{predicted}$, $R^2_{adjusted}$ and $Adeq_{precision}$ values. Diagnostics such as NPR (normal plot of residuals), RVP (residuals versus predicted), RVR (residuals versus run), RVF (residuals versus factors) and PVA (predicted versus actual) were also examined to statistically validate the models. Once the models were validated, numerical optimization tool was implemented to obtain the optimum values of pyrolysis parameters (Py_T and Py_t) and biochar properties (BC_Y, BC_{SA} and BC_{PV}) by fixing the optimizing criteria. Option for selecting the optimizing criteria such as maximize, minimize, target, in range, and equal to be provided in the software. The effect of pyrolysis parameters on biochar properties was shown using 3D response surface plots and 2D contour plots while the optimized parameters were illustrated as ramps.

Characterization of ZLD sludge biochar

ZLD sludge biochar yield (%) was found using the relation: (ZLD sludge biochar mass ÷ ZLD sludge mass) × 100. BC_{SA} and BC_{PV} were measured using Quanta chromeAutosorb automated gas adsorption apparatus. The proximate analysis namely ash (%), moisture (%), and volatile matter (%) was determined using ASTM D1102-84, ASTM E871-82, and ASTM E872-82 respectively while the fixed carbon (%) was calculated using the relation (100 – ash – moisture – volatile matter). The elemental proportion of C (carbon, %), H (hydrogen, %), N (nitrogen, %), and S (sulphur, %) was analysed using an elemental analyser (Vario EL 111, Elementar). The O (oxygen, %) content was calculated using relation O = 100 - (C + H + N + ash) [16].The thermal analysis of the ZLD sludge biochar was determined by using a DSC-TGA thermal analyzer with a heating rate of 10°C and temperature range 430°C–600°C. The obtained results are given in results and discussion section (Fig. 8). Identification of the functional group of the ZLD sludge biochar was analyzed using FT-IR (Perkin Elmer model, USA) spectroscopy in the wavelength range of 400-4000 cm^{-1}. The surface morphology of the ZLD sludge biochar was inspected using SEM (Zesiss model, EVO LSIS, German). XRD (Rigaku Miniflex-600, Japan) patterns of ZLD sludge biochar were also recorded.

RESULTS AND DISCUSSION

Model for ZLD sludge biochar yield, surface area and pore volume

The statistical models describing the relation between pyrolysis temperature, pyrolysis time, and ZLD sludge biochar yield, surface area, and pore volume are shown in the following equations:

$$BC_Y = 56.36 - 7.08Py_T + 2.84Py_t + 1.80Py_T^2 + 0.88Py_t^2 + 1.05Py_TPy_t \quad (2)$$

$$BC_{SA} = 57.34 + 14.44Py_T - 3.46Py_t - 10.19Py_T^2 - 8.26Py_t^2 - 9.18Py_TPy_t \quad (2)$$

$$C_{PV} = 0.0576 + 0.0100Py_T - 0.0054Py_t - 0.0067Py_T^2 - 0.0037Py_t^2 - 0.0115Py_TPy_t \quad (4)$$

These equations have been derived using coded values of temperature and time. This can be employed for predicting response that provided levels of Py_T and, Py_t. By default, the high and low levels of Py_T and, Py_t have been coded +1 and -1 respectively while the centre and factorial levels are coded 0 and ±1.414, respectively. The coded equation helps in ascertaining the comparative effect of the variables by matching the coefficients of the factors involved.

The ANOVA of these equations are presented in Table 2. The results ascertained that the BC_Y, BC_{SA} and BC_{PV} models are significant with an F value of 81.10, 42.36 and 36.37, respectively. There is only a chance of 0.01 that such a large F value could appear due to noise. P values < 0.05 designate that model values are important. In BC_Y model, only Py_T, Py_t and Py^2_T are the key parameters while in BC_{SA} and BC_{PV} models all the terms i.e. Py_T, Py_t, Py_T^2, Py_t^2 and Py_TPy_t are important. Values > 0.1000 indicate that model values are unimportant. If there are several non-essential model parameters, their exclusion can refine the model. The $F\text{-}value_{LOF}$ of 2.31, 5.19 and 3.33 respectively, in BC_Y, BC_{SA} and BC_{PV} models means these are not significant with respect to the error. There is respectively 21.84%, 7.27% and 13.81%possibility that these big $F\text{-}value_{LOF}$ may be due to noise. The insignificant LOF in these cases are good because they show a suitable model [15, 17]

The $R^2_{predicted}$ values for BC_Y, BC_{SA} and BC_{PV} models are0.9138, 0.8087 and 0.7953, respectively. This is in accord with respective $R^2_{adjusted}$ values of 0.9709, 0.9451 and 0.9365.Since the difference between these two values i.e. ($R^2_{adjusted} - R^2_{prediced}$) is below 0.2. $Adeq_{precision}$ Values measure the average audio rating. A rating greater than 4 is attractive. A rating of 29.158, 18.826, and 19.909 respectively for these models indicates a sufficient signal. These models work well for navigating the concerned design space. In equation (2) the coefficient of Py_T shows a negative sign while others show a positive sign but in equation (3) and (4) the coefficient of Py_T shows a positive sign while others show a negative sign. The positive (+) and the negative (-) sign of the coefficient respectively correlate with the boost and the decline in output when the process value accentuates [15]. This implies that with the increase in pyrolysis temperature the yield of ZLD sludge biochar decreases while the surface area and pore volume of ZLD sludge biochar increases.

The other diagnostics of BC_Y, BC_{SA} and BC_{PV} models such as NPR, RVP, RVR, RVF (i.e., residuals versus pyrolysis temperature and residuals versus pyrolysis time) and PVA is shown in Figs. 2, 3, and 4, respectively. The decrease in biochar yield with process temperature and time associated with volatile matter liberation. And an identical effect is detected while increasing pyrolysis temperature and pyrolysis time. This is because at elevated temperature Py_T the internal and surface morphology of biochar altered significantly. These figures suggest that the residuals are normally distributed with a straight line and these are haphazardly scattered across the x-axis without a definite pattern. All the aforementioned diagnostics confirmed that the BC_Y, BC_{SA} and BC_{PV}models are well fit in terms of pyrolysis temperature and time. These models can perform better to explain the slow pyrolysis process adopted for the preparation of ZLD sludge biochar. Also, the properties of ZLD sludge biochar can be predicted well with the help of these models.

Effect of pyrolysis temperature and time on ZLD sludge biochar yield, surface area and pore volume

Fig. 5 (a) and (d) shows the surface and contour plots for BC_y model. It can be noted that with increasing pyrolysis temperature the yield of ZLD sludge biochar decreases while as the pyrolysis period increases the yield of ZLD sludge biochar decreases. It can be noted that the structure of the contour structure is not very elliptical. This shows that the link between pyrolysis temperature and pyrolysis temperature is not important. It is also indicated by the p value of the term Py_TPy_t in the variance analysis [18]. The fall off biochar yield with escalating Py_T is associated with substantial liberation of volatile matters. An identical effect is observed with increasing Py_t across same Py_T (but at lower Py_T) [19]. This is due to the fact that at elevated Py_T the surface and internal morphology of biochar gets significantly altered.

Fig. 5 (b) and (e) illustrates the surface and contour plots generated for BC_{SA} model. It can be noted that with the increase in Py_T surface area of ZLD sludge biochar first increases and after some time reaches the highest value and thereafter remains almost constant while with the increase in pyrolysis time surface area of ZLD sludge

Table 2: Analysis of variance table for biochar yield.

Source	Sum of squares	df	Mean square	F-value	p-value	Remarks
BC_Y model						
Model	496.15	5	99.23	81.10	<0.0001	Significant
Py_T	401.44	1	401.44	328.11	<0.0001	
Py_t	64.74	1	64.74	52.91	0.0002	
Py_TPy_t	4.39	1	4.39	3.59	0.1000	
Py^2_T	22.59	1	22.59	18.46	0.0036	
Py^2_t	5.45	1	5.45	4.45	0.0728	
Residual	8.56	7	1.22			
Lack of Fit (LOF)	5.43	3	1.81	2.31	0.2184	Not Significant
Pure error	3.14	4	0.7844			
Cor Total	504.71	12				
BC_{SA} model						
Model	3164.89	5	632.98	42.36	< 0.0001	Significant
Py_T	1669.11	1	1669.11	111.69	< 0.0001	
Py_t	95.82	1	95.82	6.41	0.0391	
Py_TPy_t	337.11	1	337.11	22.56	0.0021	
Py^2_T	722.62	1	722.62	48.35	0.0002	
Py^2_t	475	1	475	31.78	0.0008	
Residual	104.61	7	14.94			
Lack of Fit	83.24	3	27.75	5.19	0.0727	Not significant
Pure error	21.38	4	5.34			
Cor Total	3269.51	12				
BC_{PV} model						
Model	0.0019	5	0.0004	36.37	<0.0001	Significant
Py_T	0.0008	1	0.0008	75.49	<0.0001	
Py_t	0.0002	1	0.0002	21.81	0.0023	
Py_TPy_t	0.0005	1	0.0005	49.99	0.0002	
Py^2_T	0.0003	1	0.0003	29.29	0.0010	
Py^2_t	0.0001	1	0.0001	8.88	0.0205	
Residual	0.0001	7	0.0000			
Lack of Fit	0.0001	3	0.0000	3.33	0.1381	Not Significant
Pure error	0.0000	4	5.300E-06			
Cor Total	0.0020	12				

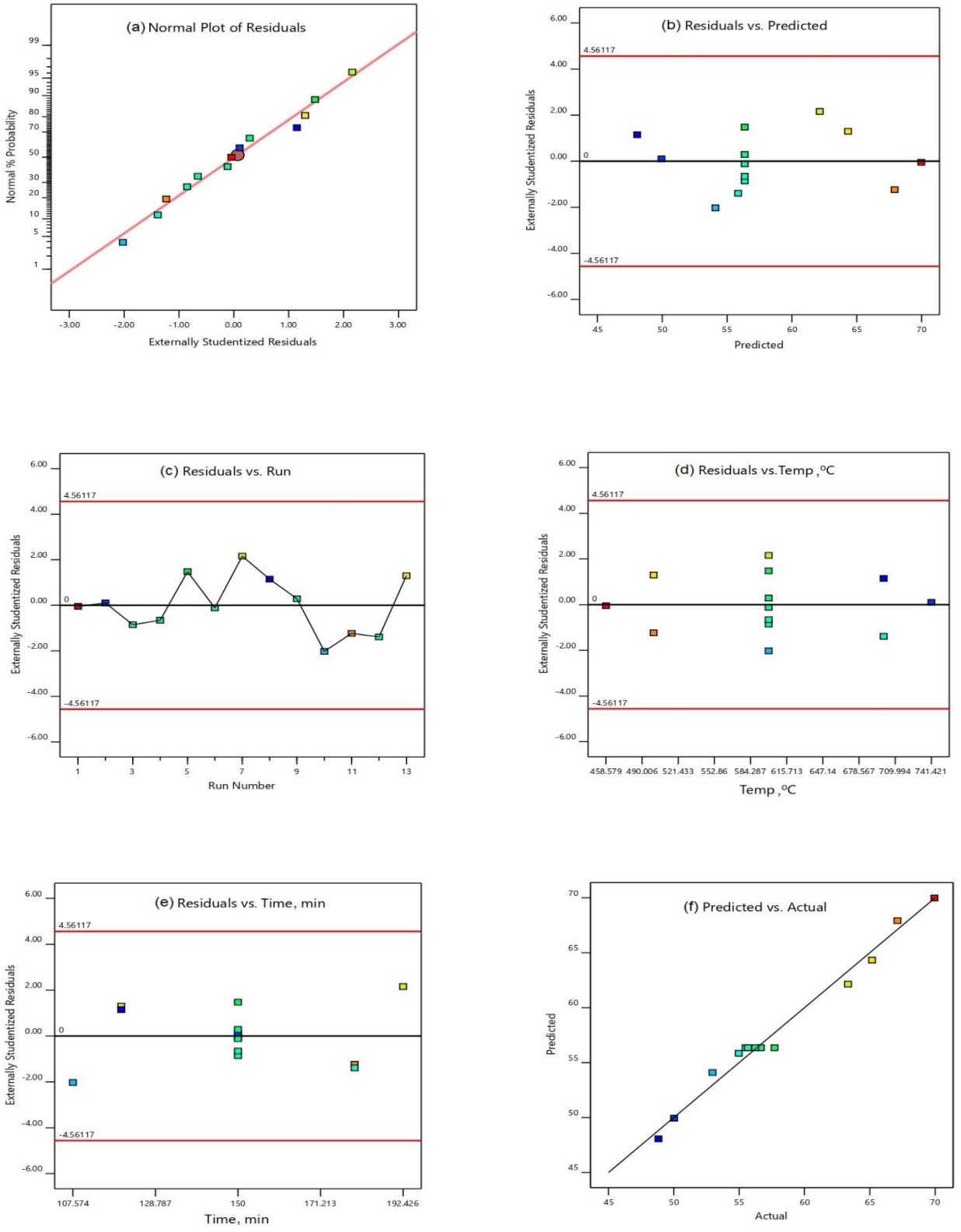

Fig. 2: BCY model diagnostics (a) NPR, (b) RVP, (c) RVR, (d) Residuals versus pyrolysis temperature, (e) Residuals versus pyrolysis time, (f) PVA.

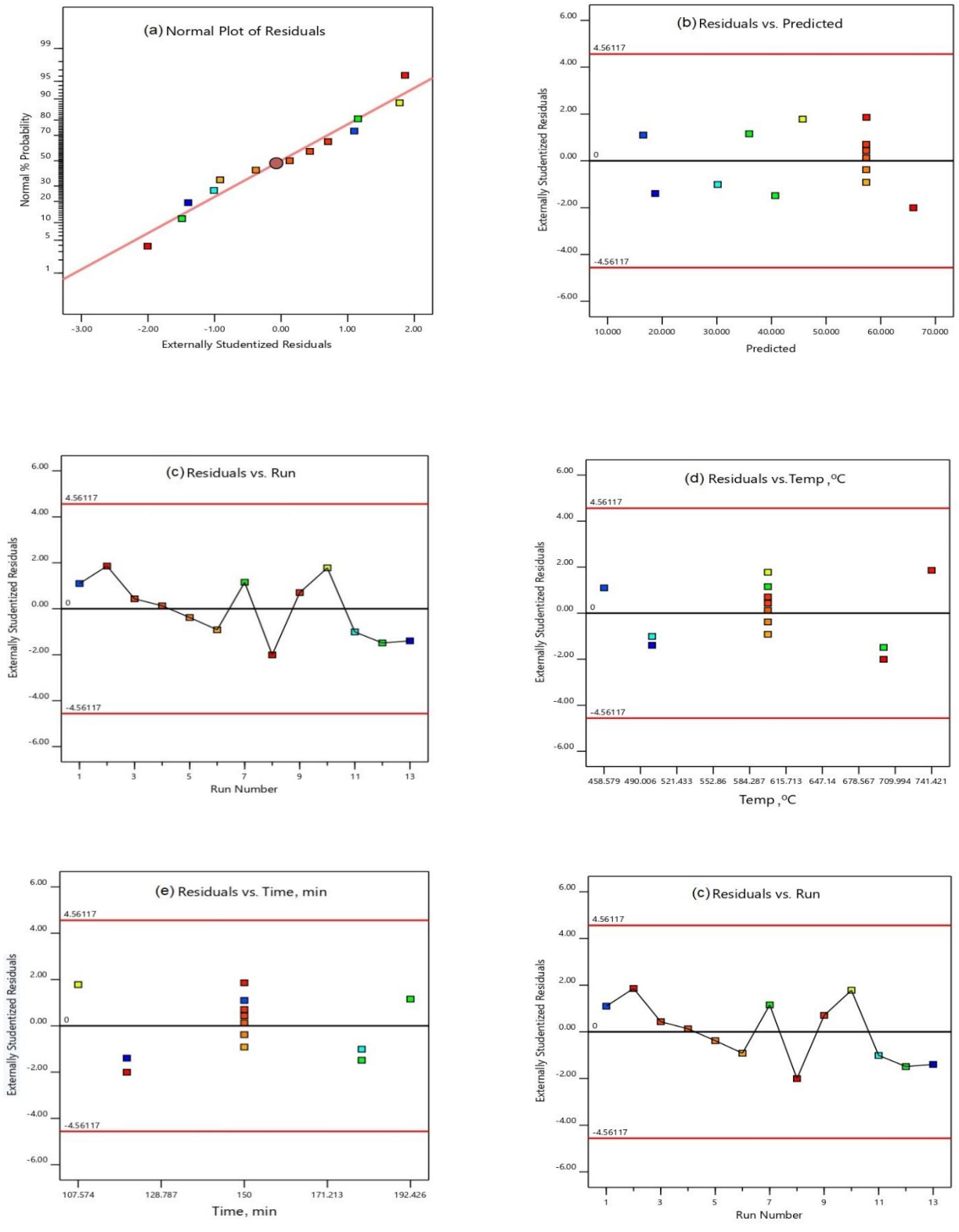

Fig.3: BCSA model diagnostics (a) NPR, (b) RVP, (c) RVR, (d) Residuals versus pyrolysis temperature, (e) Residuals versus pyrolysis time, (f) PVA.

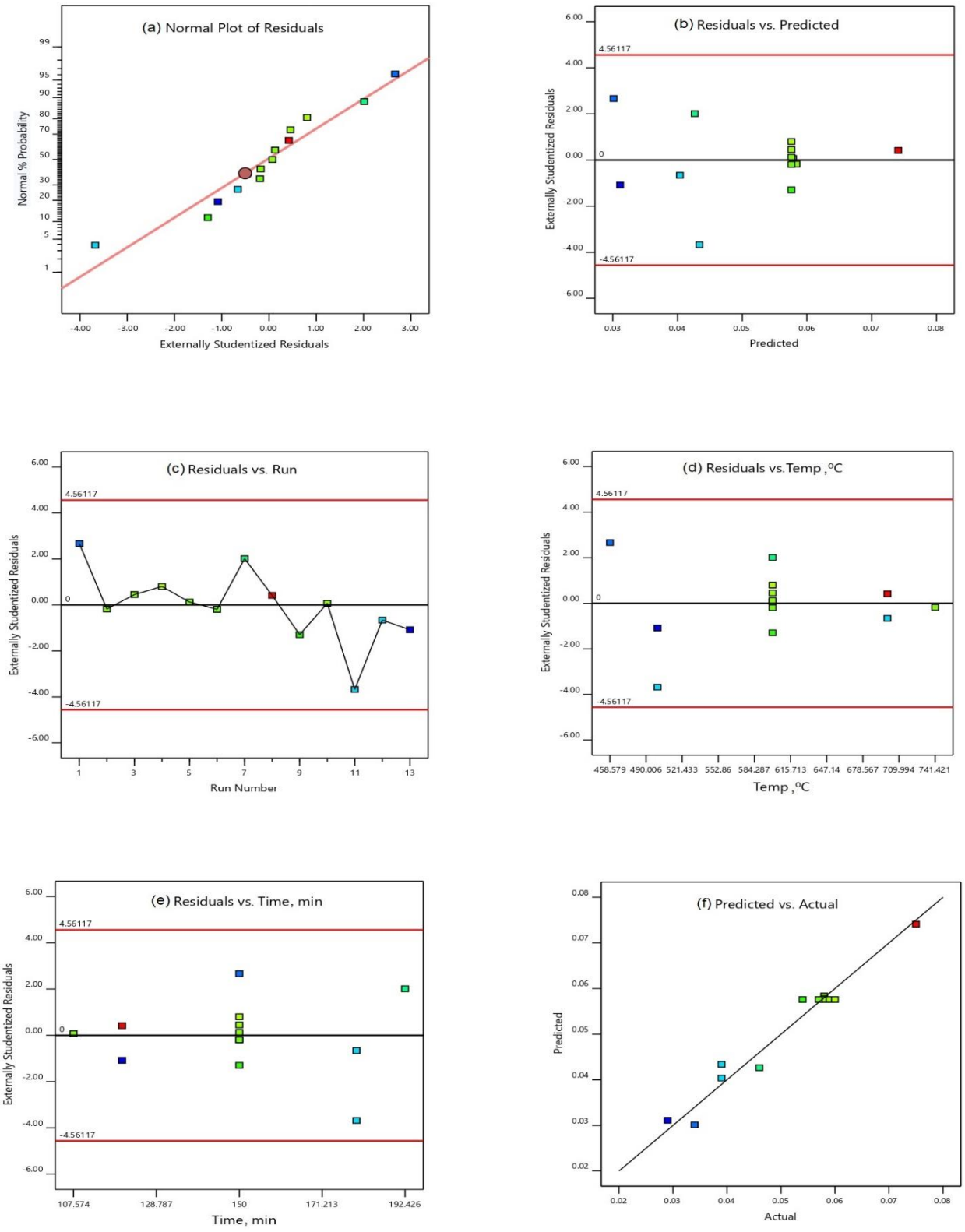

Fig. 4: BCPV model diagnostics (a) NPR, (b) RVP, (c) RVR, (d) Residuals versus pyrolysis temperature, (e) Residuals versus pyrolysis time, (f) PVA.

biochar first increases and after some time reaches the highest value and thereafter starts decreasing. It can be noticed that the shape of the contour plot is perfectly elliptical. This shows that the interaction between Py_T and Py_t is very much significant. It is also reflected by the *p*-value of Py_TPy_t term (< 0.05) in the analysis of variance [20, 17]. Fig. 5 (c) and (f) illustrate surface and contour plots drawn for BC_{PV} model. It is obvious that with the augmentation in pyrolysis temperature pore volume of ZLD sludge biochar increases throughout while with the escalating pyrolysis time pore volume of ZLD sludge biochar shows a continuous decreasing trend. It can be noticed that the shape of the contour plot is also perfectly elliptical. This shows that there is a significant interaction between pyrolysis time and temperature. It is also reflected by the *p*-value of Py_TPy_t term (< 0.05) in the analysis of variance [21, 22]. In his review on the effect of pyrolysis temperature on biochar physicochemical characteristics reported that with the rise in Py_T organic matter, aromatic lignin, aliphatic alkyls, and ester groups decompose/destruct. This leads to the development of a higher surface area, porosity, and formation of microspores. Also, it has been observed that the liberation of volatile matters at higher Py_T causes the generation of plentiful pores. The evolution of the higher surface area and substantial pores make the adsorbent, here paper mill ZLD sludge, is more efficient in the adsorptive treatment of organic/inorganic pollutants.

Optimum parameters of ZLD sludge biochar

The optimum condition of pyrolysis temperature and time was determined using the numerical optimization option provided by Design-Expert software. This optimization technique is based on the desirability approach [15]. The optimization of the pyrolysis process aimed to minimize pyrolysis temperature while maximizing pyrolysis time, ZLD biochar yield, surface area, and pore volume. The temperature opted to minimize while time was opted to maximize because it has been found that lower pyrolysis temperatures sat longer pyrolysis times facilitate biochar production. Higher yield makes biochar production commercially more cost-efficient while the larger values of surface area and pore volume favor the adsorption process [15, 17, and 22]. The optimum conditions were estimated to be pyrolysis temperature 539.65°C and pyrolysis time 176.67 min with desirability 0.651. The optimum yield, surface area, and pore volume were measured to be 63.95%, 40.23 m^2/g, and 0.048 cm^3/g respectively. The ramps for the numerical optimization have been shown in Fig. 6. Here, Py_T has higher desirability than Py_t. The desirability for ZLD sludge biochar quality can be placed in increasing order as $BC_{PV} < BC_{SA} < BC_Y$

Physicochemical characteristics of ZLD sludge biochar

Proximate and ultimate analysis

The proximate analysis involves the measurement of the volatile matter, moisture, ash, and fixed carbon contents of biochar. Table 3 provides the proximate analysis results of ZLD sludge biochar. It also compares these components of ZLD sludge biochar with other biochar reported in the literature. The volatile matter of ZLD sludge biochar is higher as compared to that of palm oil sludge and charcoal, similar to that of apricot stone but lower than the remaining. Its moisture content is analogous to that of groundnut shell and soybean Stover, above that of peanut shell but below that of palm oil sludge and food waste – sewage sludge mixture. Its ash content is the highest of all except palm oil sludge. On the other hand, the fixed carbon content is similar to that of palm oil sludge, higher than that of the lowest of all except that of groundnut shell. The proximate results in this study are consistent with the literature that suggests that biochar exhibits <30% fixed carbon if it has an ash content of >35% [23]. VM/FC ratio of paper mill ZLD sludge is greater than that of palm oil sludge, apricot stone, and charcoal while lower than the others. VM/FC of a biochar suggests its stability and quality [24]. The lower the VM/FC value, the better the stability and the quality of the biochar. It is to be noted that in addition to the nature of feedstock, VM/FC also depends on the type of pyrolysis i.e., whether slow pyrolysis or fast pyrolysis has been used to prepare biochar [25].

The carbon, hydrogen, nitrogen, sulfur, and oxygen composition of ZLD sludge biochar is presented in Table 4. It also compares this elemental composition of ZLD sludge biochar with other biochar reported in the literature. The carbon-hydrogen, nitrogen, and oxygen content of ZLD sludge biochar were calculated to be 14.98 %, 0.363, 0.385, and 0.825 % respectively. High carbon content in ZLD sludge biochar confirms the purity of biochar [31]. Table 5 shows that carbon present in the paper mill ZLD

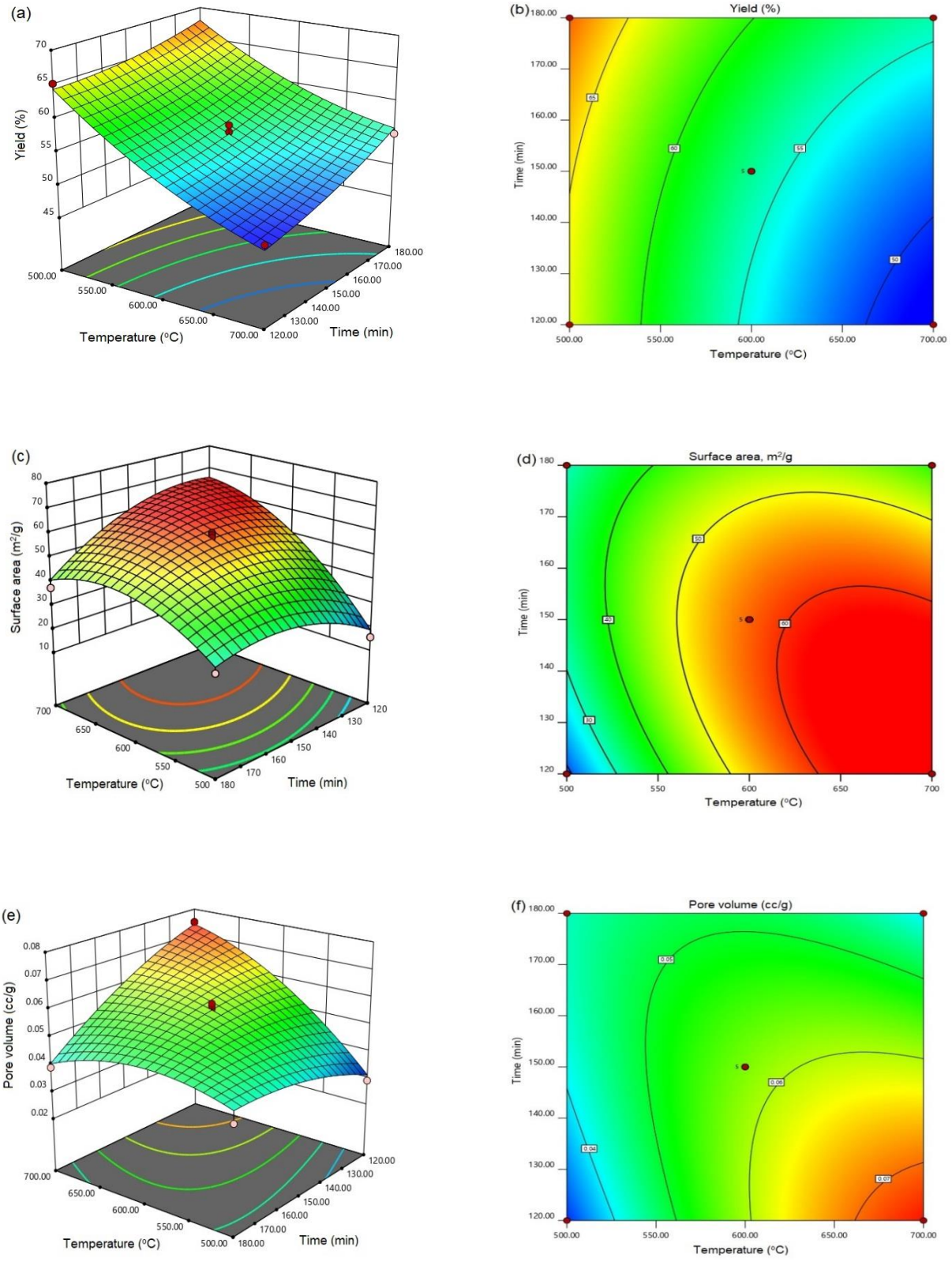

Fig.5: (a, c, e) response surface, (b, d, f) contour diagram for ZLD sludge biochar yield, surface area, and pore volume

Table 3:Proximate analysis of ZLD sludge biochar and its comparative assessment.

Raw material	VM	M	AS	FC	VM/FC	Reference
Palm oil sludge	14.51	6.73	49.14	29.62	0.490	[34]
Apricot stone (Dry basis)	19.83	-	8.47	71.70	0.277	[26]
Peanut shell	60.47	1.29	1.24	37	1.63	[27]
Groundnut shell	79.54	4.54	1.79	14.13	5.629	[28]
Food waste - sewage sludge mixture	77.20	7.07	3.09	19.70	3.919	[29]
Charcoal (Dry basis)	9.88	-	1.02	89.10	0.111	[30]
Soybean Stover	46.34	4.50	10.41	-	1.195	[27]
Grape seed (Dry basis)	39.45	-	9.59	50.96	0.774	[26]
Paper mill ZLD sludge (Dry basis)	19	5	47	29	0.655	This Paper

VM: Volatile Matter; M: Moisture; FC: Fixed carbon; AS: Ash. All measured in %.

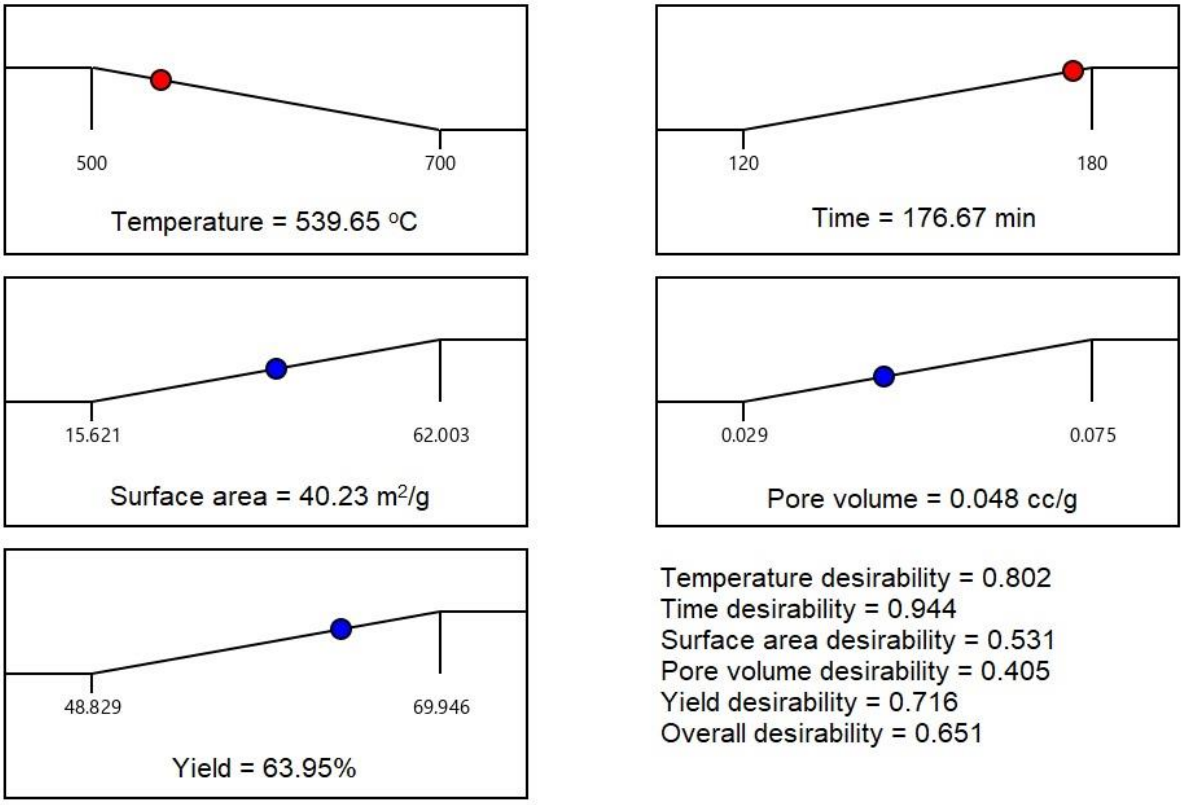

Fig.6: Desirability ramp for the numerically optimized Py_T, Py_t, BC_Y, BC_{SA}, and BC_{PV}.

sludge biochar is comparatively low as compared to the biochar prepared from sewage sludge, palm oil sludge, and activated petroleum sludge. ZLD sludge biochar possesses nitrogen content similar to that of switchgrass but more than that of bamboo sludge and lower than that of sewage sludge, peanut shell, and soybean Stover. Hydrogen and oxygen content is the lowest among all. Sulfur content is similar to that of activated sewage sludge and activated petroleum sludge but less than that of sewage sludge. Molar ratios of elements such as O/C and H/C have been used to evaluate polarity, carbonization degree, and development of aromaticity of biochar [32]. The accepted

Table 4: Ultimate analysis of ZLD sludge biochar and its comparative assessment.

Raw material	C	H	N	S	O	O/C	H/C	N/C	Reference
Switch grass (Dry basis)	43.20	6.20	0.47	-	44	1.02	0.14	0.01	[33]
Palm oil sludge (Dry basis)	30.05	2.60	3.88	0.49	-	-	0.09	0.13	[34]
Sewage sludge (Dry basis)	27.06	12.51	4.24	2.12	-	-	0.46	0.16	[35]
Activated Petroleum waste sludge (Dry basis)	36.8	6.30	4.23	1.81	23.3	0.63	0.17	0.11	[61]
Peanut shell	68.27	3.85	1.91	0.09	25.89	0.38	0.06	0.03	[27]
Sewage sludge mixed with Cotton stalks (Dry basis)	36.98	2.82	2.86	-	21.92	0.59	0.07	0.08	[36]
Bamboo	46.52	6.11	0.20	-	46.89	1.01	0.13	0.004	[37]
Soybean Stover (Dry basis)	68.81	4.29	1.88	0.04	24.99	0.36	0.06	0.03	[27]
Sewage sludge activated (Dry basis)	48.42	7.03	7.53	1.54	-	-	0.14	0.15	[38]
Paper mill ZLD sludge (Dry basis)	14.98	0.363	0.385	1.271	0.825	0.05	0.02	0.02	This Paper

value of the O/C and H/C ratio in biochar should be below 0.4 and 0.6, respectively. This is confirmed by the elemental composition of ZLD sludge biochar. The O/C and H/C ratios were obtained respectively to be 0.38 and 0.04 in a peanut shell, 0.59 and 0.07 in sewage sludge mixed with cotton stalk, and 0.36 and 0.06 in soybean Stover.

Characterization results

X-ray diffraction and Fourier Transform Infra-Red spectroscopy

The XRD pattern of ZLD sludge biochar is shown in Fig. 6 (a). XRD is an appropriate technique for analyzing the biochar crystallinity and the biochar structure. Higher pyrolysis temperature with longer retention time possibly will facilitate the development of crystalline structure [39].Two narrow sharp peaks at the 2 theta values around 26.61°and 29.38° can be allocated to the crystalline region of ZLD sludge biochar. Some other broad peaks at 23.03°, 31.35°, 35.97°, 39.39°, and 43.13° were exhibited in biochar and it confirms its crystallinity [40]. The FT-IR spectra of ZLD sludge biochar are shown in Fig. 6(b). The spectra of the biochar are identified by various principal bands. The various peaks arise such as 3881 cm-1, 3760 cm-1and 3430 cm^{-1} due to hydrogen-bonded –OH stretching of phenol. The absorbance peaks arise around 2925 cm^{-1} and 2856 cm^{-1} signifies the aliphatic C-H stretch vibration in the ZLD sludge biochar. Important peaks exhibit of the ZLD sludge biochar containing C-H stretch around 875 cm^{-1}, 712 cm^{-1}, and the aromatic C-C stretch at 1623 cm^{-1}. This clearly shows an increment in the degree of condensation and aromaticity of the biochar. Similar results were obtained for bamboo biochar, sugarcane biochar, neem biochar, plastic biochar [41], textile sludge biochar [42], and Pinusbanksian [43]. The ZLD sludge biochar exhibited a distinct peak at 1017 cm^{-1}. This peak corresponds to the C-O stretching from carbohydrates. The peak at 1433 cm^{-1} confirms the O-H bending carboxyl group in biochar [44].

Scanning electron microscopy, thermos gravimetric, and differential scanning calorimetry analysis

Fig. 7 (a) and 7 (b) represent the micro surface structure of ZLD sludge biochar with 50 and 100 magnifications respectively. These figures show porous structure on a rough surface [45]. ZLD biochar sludge with an average dimension of around 1µm can be found using high magnification. At high magnification, it was observed that the dimensions as well as pore of the ZLD biochar increase after pyrolysis. The similar study was reported in the literature [46, 47].The thermal stability of ZLD sludge biochar was determined by DSC and TGA [48]. Fig. 8(a) shows the heating/melting curves and latent heat from DSC measurement of the ZLD sludge biochar. The peak melting temperatures were 154.59 °C, 191.24 °C, and 301.22 °C. At these temperature values, the DSC heat values (w/g) were negatives it indicating that the charging process was endothermic. The latent heat values were found to be 3.82 J/g, 32.11 J/g, and 13.82 J/g at corresponding temperatures [49]. TGA plot is shown

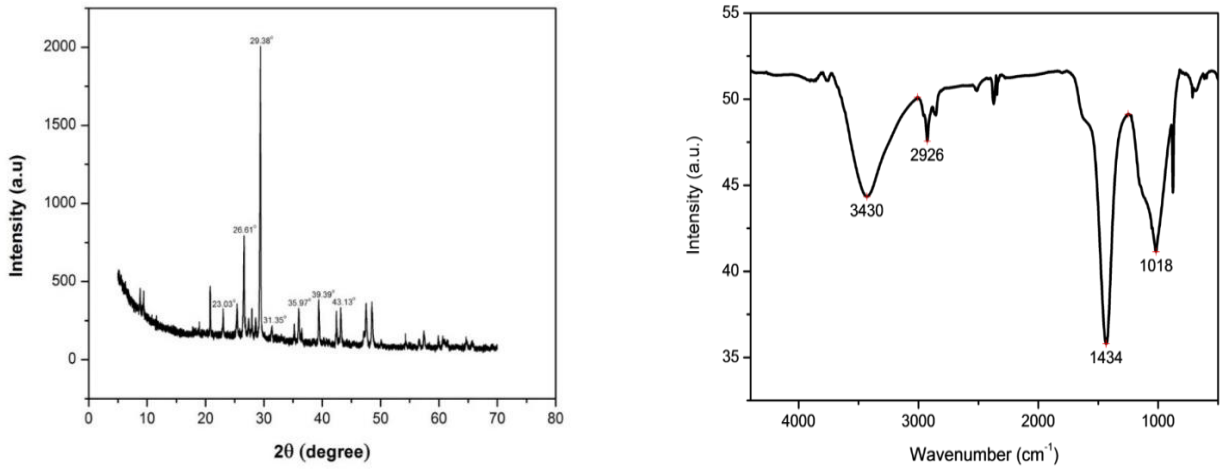

Fig. 6: (a) XRD spectrum and (b) FT-IR plot of ZLD sludge biochar.

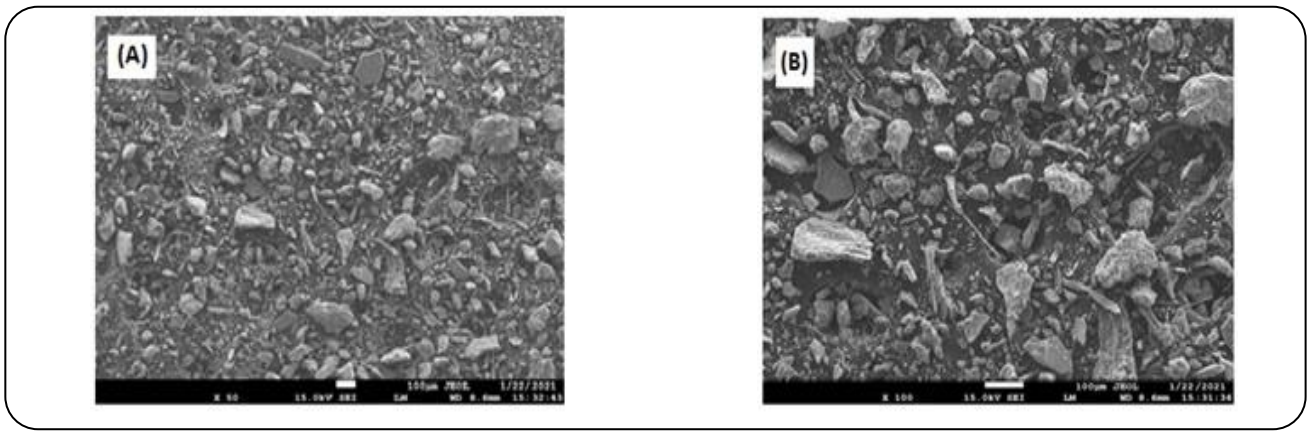

Fig. 7: SEM images of ZLD sludge biochar (a) at 50X, and (b) at 100X.

in Fig. 8. The TGA curve of ZLD sludge biochar was identified by steady loss in weight with temperature and a constant decrease in weight was noticed. Some peaks were arising confirms the loss of moisture and maximum loss occurred because of emission of gases such as CO, CO_2, and CH_4 and breakdown of organic compounds. After that, a constant and slow decline in the spectra was also observed. The steady weight loss normally takes place in the carbonization stage, where the thermal breakdown of solid matter (char and inorganic matter) occurred leading to conversion of sludge to solid biochar which has stable carbon [50,48]

In Fig. 9, surface area and pore volume of 13 samples are plotted which are extracted from BET results. Here in this plot sample-1 shows maximum surface area and pore volume and after they start decreasing and follow a random order. From this graph we have obtained the optimized result.

Comparative assessment of optimized ZLD sludge biochar parameters

The optimal temperature, time, yield, pore volume, and surface area for ZLD sludge biochar were compared to those reported in the literature to assess the feasibility of the biochar preparation process used in this work as well as the quality of ZLD sludge biochar generated. The comparison of optimum pyrolysis settings and ZLD sludge biochar characteristics is shown in Table 5. The majority of sludge samples in the literature have been pyrolyzed at temperatures ranging from 500 to 900°C for 1 to 3 hours at a heating rate of 5 to 20°C /min. Though there are instances in the literature that palm oil sludge, iron-loaded sludge, sewage sludge, and paper mill sludge were pyrolyzed at 300–442°C, 180°C, 300°C, and 315°C, respectively, which is around 500°C. Except for rapeseed, walnut shell,

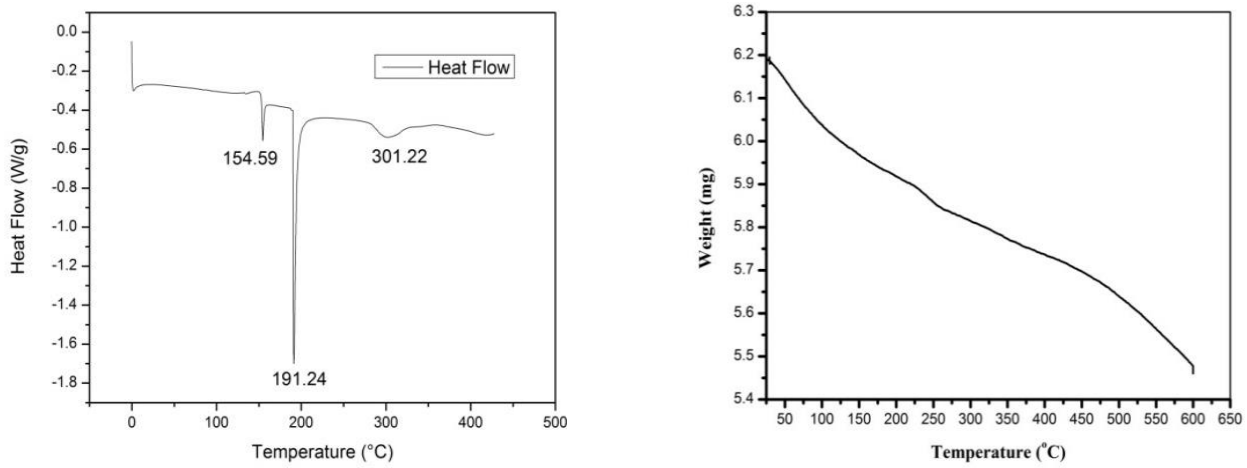

Fig. 8: (a) DSC graph and (b) TGA curve of ZLD sludge biochar.

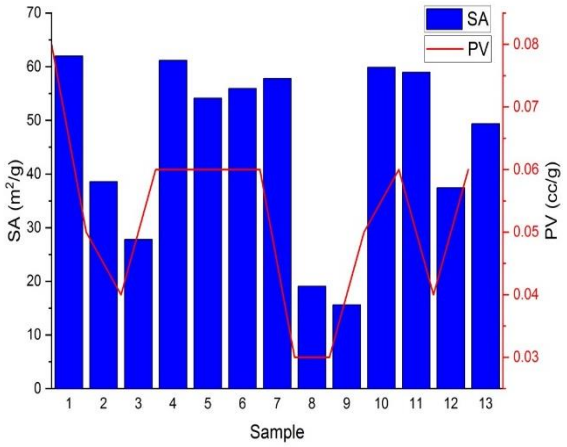

Fig. 9: (a) BET graph of ZLD sludge biochar

and other lignocellulosic wastes, which were pyrolyzed at 600–700ºC for biochar formation, biomass materials were pyrolyzed at 500ºC. ZLD sludge has a lower optimum pyrolysis temperature than municipal sewage sludge, dolomite modified sewage sludge, sewage sludge mixed with cotton stalks, activated petroleum waste sludge, and sewage sludge activated walnut shell, rapeseed, and some lignocellulosic wastes, but a higher optimum pyrolysis temperature than the rest. The lower pyrolysis temperature means less energy is consumed during the process, resulting in cheaper biochar manufacturing costs. The optimum heating rate is the highest of all and the same as that of palm oil sludge. A sufficient pyrolysis time is needed for the chemistry behind reactions involved in biochar production.

Paper mill ZLD sludge biochar yields are comparable to municipal sewage sludge lower than chicken manure, fescue straw, and tire rubber, but higher than the rest. A larger biochar yield proves its commercial viability by making the biochar production process more cost-effective. The surface area of ZLD sludge from a paper mill is smaller than that of palm oil sludge, activated petroleum waste sludge, iron-loaded sludge, soybean Stover, active sewage sludge, walnut shell, and sawdust, but larger than the rest. The pore volume of paper mill ZLD sludge biochar is comparable to maize Stover and modified rice straw, but smaller than that of switchgrass. miscanthus, and activated petroleum waste sludge while larger than the rest. A higher surface area and pore volume of carbon-based adsorbent is sought for its efficient performance towards the adsorptive treatment of wastewater [51]. These comparative tables indicate that the biochar prepared from paper mill ZLD sludge in this study is better than many of the biochar reported in the literature in the light of surface area, yield, and pore volume. Even the pyrolysis temperature and time are either analogous or better to others.

CONCLUSIONS

This paper describes the preparation of biochar from sludge generated in pulp and paper mills that operate on the ZLD concept. Biochar prepared through slow pyrolysis at 539.65°C for 176.67 min with heating rate 20ºC/min exhibited surface area 40.23 m^2 /g, yield 63.95%, and pore volume 0.048cc/g. The polynomial models formulated

Table 5: Comparison of ZLD sludge biochar parameters with literature data.

ZLD sludge biochar yield			
Raw material	Pyrolysis condition	Biochar Yield (%)	Reference
Peanut shell	300, 7ºC/min,3h	36.9	[27]
Municipal sewage sludge	500ºC,900ºC	63.10,53.31	[52]
Sugarcane bagasse	400ºC, 10ºC/min,2h	31.6	[53]
Chicken Manure	350ºC, 1.67ºC/min,0.5h	69.7	[54]
Prosopis Africana shell	350ºC	60.05	[55]
Fescue straw	100ºC, 1h	99.9	[56]
Tire rubber	200ºC, 10ºC/min,2h	93.5	[57]
Cottonseed hull	350ºC, 4h	36.8	[58]
Bamboo	450ºC	26.3	[59]
Buckwheat husk	350ºC, 10ºC/min,4h	46.3	[60]
Paper mill ZLD sludge	539.65ºC, 2.94h, 20ºC/min	63.95	This study
ZLD sludge biochar surface area			
Raw material	Pyrolysis condition	Surface Area (m^2/g)	Reference
Palm oil sludge	300ºC, 442ºC,20ºC/min	61.4,74.9	[34]
Dolomite modified Sewage sludge	800°C, 5ºC/min,2h	11.31	[38]
Sewage sludge mixed with Cotton stalks	600°C, 1.5h	31.33	[36]
Activated Petroleum waste sludge	850°C, 10ºC/min,1h	143	[61]
Poultry litter	450°C,550°C, 40min	5.65,18.12	[62]
Iron Loaded sludge	180°C, 3h	82.78	[63]
Sewage sludge	300°C,500°C, 3h	0.71,3.77	[35]
Fe-Zn-P modified sludge	500°C, 10ºC/min,2h	14	[64]
Soybean Stover	300°C, 7ºC/min,3h	420.3	[27]
Sewage sludge activated	700°C, 10ºC/min,1h	81.35	[65]
Walnut shell	573-873ºC,3h	292.58	[66]
Paper mill sludge	315°C,150min	3.43	[67]
Paper mill ZLD sludge	539.65ºC, 2.94h, 20ºC/min	40.23	This study
ZLD sludge biochar pore volume			
Raw material	Pyrolysis condition	Pore Volume (cc/g)	Reference
Switch grass	500ºC, 20ºC/min, 2h	0.06	[17]
Corn Stover	500ºC,20ºC/min, 2h	0.05	[17]
Activated Petroleum waste sludge	850°C, 10ºC/min,1h	0.20	[61]
Corn straw	400°C,1.5h	0.008	[68]
Rapeseed	500ºC,700ºC, 7ºC/min	0.03,0.04	[69]
Lignocellulosic wastes.	300ºC,700ºC,10ºC/min,2h	0.0057,0.031	[70]
Peanut shell	400°C,1.5h	0.007	[68]
Paper mill sludge	315°C, 2.5h	0.02	[67]
Safflower seed press cake	400ºC ,500ºC,10ºC/min	0.005,0.008	[69]
Wheat straw	400°C,1.5h	0.012	[68]
Modified rice straw	50°C,10ºC/min	0.055	[71]
Paper mill ZLD sludge	539.65ºC, 2.94h, 20 ºC/min	0.048	This study

through response surface methodology for biochar preparation are well fit. The $R^2_{prediced}$ values for BC_Y, BC_{SA} and BC_{PV} models were 0.9138, 0.8087 and 0.7953, respectively. These models can effectively predict the yield, surface area, pore volume of paper mill ZLD sludge biochar within the selected range of pyrolysis temperature and time. These models also account well for the interactive, synergistic, and antagonistic effect of pyrolysis parameters towards the ZLD biochar preparation. Also, the numerical optimization technique adopted in this study was found suitable in optimizing the ZLD sludge pyrolysis process. A comparison of optimum pyrolysis parameters, surface area, yield, and pore volume of paper mill ZLD biochar with those of biochar produced from different types of sludge and biomass revealed that the former is at par in quality.

Nomenclatures

Py_T	Pyrolysis temperature
Py_t	Pyrolysis time
BC_Y	Biochar yield
BC_{SA}	Biochar surface area
BC_{PV}	Biochar pore volume
CO_2	Carbon dioxide
H_2O	Water
C	Carbon
H	Hydrogen
N	Nitrogen
O	Oxygen
S	Sulphur
M	Moisture
AS	Ash
VM	Volatile matter
FC	Fixed carbon
ZLD	Zero liquid discharge
RCF	Recycled fiber
WW	Wastewater
ETP	Effluent treatment plant
PPMs	Pulp and paper mills
NPR	Normal plot of residuals
RVP	Residuals versus predicted
RVR	Residuals versus run
PVA	Predicted versus actual
LOF	Lack of fit
RSM	Response surface methodology
ANOVA	Analysis of variance

Acknowledgements

Amit Kumar sincerely acknowledges Ministry of Human Resource and Development (MHRD), India for providing fellowship to pursue this PhD research work.

Received : Oct. 20, 2021 ; Accepted : Jan. 31, 2022

REFERENCES

[1] Mehmood K., Rehman S.K.U., Wang J., et al., Treatment of Pulp and Paper Industrial Effluent Using Physicochemical Process for Recycling, *Water (Switzerland)*, **11**: 1–15 (2019).

[2] Abhijeet P., Swagathnath G., Rangabhashiyam S., et al., Prediction of Pyrolytic Product Composition and Yield for Various Grass Biomass Feedstocks, *Biomass Convers Bio Refinery*, **10**: 663–674 (2020).

[3] K. B, Cetecioglu Z., Ince O., Pollution Prevention in the Pulp and Paper Industries, *Environ Manag. Pract*, (2011) https://doi.org/10.5772/23709

[4] Sarin V., Pant K.K., Removal of Chromium from Industrial Waste by Using Eucalyptus Bark, *Bio. Resource. Technol.*, **97**: 15–20 (2006).

[5] Yaras A., Demirel B., Akkurt F., Arslanoglu H., Thermal Conversion Behaviour of Paper Mill Sludge: Characterization, Kinetic, and Thermodynamic Analyses. Biomass Conversion, *Bio. Refinery.* (2021). https://doi.org/10.1007/s13399-020-01232-9

[6] Maroneze M.M., Zepka L.Q., Vieira J.G., et al., A Tecnologia de Remoção de Fósforo: Gerenciamento do Element Emresíduosindustriais, *Rev. Ambient e Agua*, **9**: 445–458 (2014).

[7] Tarelho L.A.C., Hauschild T., Vilas-Boas A.C.M., et al., Biochar from Pyrolysis of Biological Sludge From Wastewater Treatment, *Energy Reports*, **6**: 757–763 (2020).

[8] Arun S., Kothari K., Mazumdar D., et al., "Biochar Production from Domestic Sludge: A Cost-Effective, Recycled Product for Removal of Amoxicillin in Wastewater", *IOP Conf. Ser. Mater Sci. Eng.*, **225**: 012164 (2017).

[9] Islam M.S., Kwak J.-H., Nzediegwu C., et al., Biochar Heavy Metal Removal in Aqueous Solution Depends on Feedstock Type and Pyrolysis Purging Gas, *Environ Pollution*, **281**: 117094 (2021).

[10] Palansooriya K.N., Kim S., Igalavithana A.D., et al., Fe(III) Loaded Chitosan-Biochar Composite Fibers for the Removal of Phosphate from Water, *J. Hazard Mater*, **415**: 125464 (2021).

[11] Wang Z., Miao R., Ning P., et al., A Paper Mill Sludge-Based Calcium-Containing Porous Biochar Adsorbent for Phosphorus Removal, *J. Colloid Interface Sci.*, **593**: 434–446 (2021).

[12] Jwala V.H., Vidyarthi A.K., Singh K., Techno-Economic Sustainable Option Adopting Zero Liquid Discharge in Wastepaper Based Pulp & Paper Industries, *Int. Journ. Engg. Tech. Sci. Res.*, **4**: 898–907 (2017).

[13] Abhijeet P., Swagathnath G., Rangabhashiyam S., et al., Prediction of Pyrolytic Product Composition and Yield for Various Grass Biomass Feedstocks, *Biomass Convers Biorefinery*, **10**: 663–674 (2020).

[14] Anupam K., Dutta S., Bhattacharjee C., Datta S., Optimisation of Adsorption Efficiency for Reactive Red 198 Removal from Wastewater over TiO2 Using Response Surface Methodology, *Can. J. Chem. Eng.*, **89**: 1274–1280 (2011).

[15] Anupam K., Sharma A.K., Lal P.S., et al., Preparation, Characterization and Optimization for Upgrading Leucaenaleucocephala Bark to Biochar Fuel with High Energy Yielding, *Energy*, **106**: 743-756 (2016a).

[16] Anupam K., Swaroop V., Deepika, et al., Turning Leucaenaleucocephala Bark to Biochar for Soil Application Via Statistical Modelling and Optimization Technique, *Ecol. Eng.*, **82**: 26–39 (2015).

[17] Chatterjee R., Sajjadi B., Chen W.Y., et al., Effect of Pyrolysis Temperature on PhysicoChemical Properties and Acoustic-Based Amination of Biochar for Efficient CO2 Adsorption, *Front Energy Res.*, **8**: 1–18 (2020).

[18] Tian Y., Cui L., Lin Q., et al., The Sewage Sludge Biochar at Low Pyrolysis Temperature Had Better Improvement in Urban Soil and Turf Grass, *Agronomy*, **9** (2019).

[19] Mohd. Hasan M.H., Bachmann R.T., Loh. S.K., et al., "Effect of Pyrolysis Temperature and Time on Properties of Palm Kernel Shell-Based Biochar", In: IOP Conference Series: *Materials Science and Engineering*, 1–12 (2019).

[20] Zhao S.X., Ta N., Wang X.D., Effect of Temperature on the Structural and Physicochemical Properties of Biochar with Apple Tree Branches as Feedstock Material, *Energies*, **10**: (2017).

[21] Ippolito J.A., Cui L., Kamman C., et al., Feedstock Choice, Pyrolysis Temperature and Type Influence Biochar Characteristics: A Comprehensive Meta-Data Analysis Review, *Biochar*, **2**: 421–438 (2020).

[22] Tomczyk A., Sokołowska Z., Boguta P., Biochar Physicochemical Properties: Pyrolysis Temperature and Feedstock Kind Effects, *Rev. Environ. Sci. Biotechnol.*, **19**: 191–215 (2020).

[23] Gunamantha I.M., Widana G.A.B., Characterization Potential of Biochar from Cow and Pig Manure for Geoecology Application. In: "IOP Conference Series: Earth and Environmental Science", 1–7 (2018).

[24] Aller D., Bakshi S., Laird D.A., Modified Method for Proximate Analysis of Biochar's, *J. Anal. Appl. Pyrolysis*, **124**: 335–342 (2017).

[25] Bakshi S., Aller D.M., Laird D.A., Chintala R., Comparison of the Physical and Chemical Properties of Laboratory and Field-Aged Biochars, *J. Environ. Qual.*, **45**: 1627–1634 (2016).

[26] Özçimen D., Ersoy-Meriçboyu A., Characterization of Biochar and Bio-Oil Samples Obtained from Carbonization of Various Biomass Materials, *Renew Energy*, **35**: 1319–1324 (2010).

[27] Ahmad M., Lee S.S., Dou X., et al., Effects of Pyrolysis Temperature on Soybean Stover- and Peanut Shell-Derived Biochar Properties and TCE Adsorption in Water, *Bioresour Technol.*, **118**: 536–544 (2012).

[28] Suman S., Gautam S., Biochar Derived from Agricultural Waste Biomass Act as a Clean and Alternative Energy Source of Fossil Fuel Inputs, *Energy Syst. Environ.*, **207** (2018).

[29] Jeong Y., Lee Y.-E., Kim I.-T., Characterization of Sewage Sludge and Food Waste-Based Biochar for Co-Firing in a Coal-Fired Power Plant: A Case Study in Korea, *Sustainability*, **12**: 9411 (2020).

[30] Chaiwong K., Kiatsiriroat T., Vorayos N., Thararax C., Biochar Production from Freshwater Algae by Slow Pyrolysis, *Maejo. Int. J. Sci. Technol.*, **6**: 186 (2012).

[31] Anupam K., Sharma A.K., Lal P.S., Bist V., "Physicochemical, Morphological, and Anatomical Properties of Plant Fibers Used for Pulp and Papermaking". In: Springer International Publishing Switzerland, pp. 235–248 (2016b).

[32] Mierzwa M., Krzysztof H., Marcin G., Krzysztof J., Assessment of Energy Parameters of Biomass and Biochars, Leachability of Heavy Metals and Phytotoxicity of their Ashes, *J. Mater. Cycles Waste Manag.*, **21**: 786–800 (2019).

[33] Sadaka S., Sharara M.A., Ashworth A., et al., Characterization of Biochar from Switchgrass Carbonization, *Energies*, **7**: 548–567 (2014).

[34] Ibrahim N., Sethupathi S., Goh C.L., et al., Optimization of Activated Palm Oil Sludge Biochar Preparation for Sulphur Dioxide Adsorption, *Journal of Environmental Management*, **248**: 109302 (2019).

[35] Kong L., Liu J., Zhou Q., et al., Sewage Sludge Derived Biochar's Provoke Negative Effects on Wheat Growth Related to the PTEs, *Biochem. Eng. J.*, **152**: 107386 (2019).

[36] Wang Z., Wang J., Xie L., et al., Influence of the Addition of Cotton Stalk During Co-Pyrolysis with Sewage Sludge on the Properties, Surface Characteristics, and Ecological Risks of Biochar's, *J. Therm. Sci.*, **28**:755-762 (2019).

[37] Sun Y., Gao B., Yao Y., et al., Effects of Feedstock Type, Production Method, and Pyrolysis Temperature on Biochar and Hydro Char Properties, *Chem. Egg. J.*, **240**: 574–578 (2014).

[38] Li J., Li B., Huang H., et al., Removal of Phosphate from Aqueous Solution by Dolomite-Modified Biochar Derived from Urban Dewatered Sewage Sludge, *Sci. Total. Environ.*, **687**: 460–469 (2019).

[39] Javier Ebrego et al., Structural Changes of Sewage Sludge Char During Fixed Bed Pyrolysis, *Ind. Eng. Chem. Res.*, **48**: 3211-3221 (2009).

[40] Zheng Q., Wang Z., Chen B., et al., "Analysis of XRD Spectral Structure and Carbonization of the Biochar Preparation", Guang Pu, Xue Yu, Guang Pu, Fen Xi, **36**: 3355–3359 (2016).

[41] Singh E., Kumar A., Mishra R., et al., Pyrolysis of Waste Biomass and Plastics for Production of Biochar and its Use for Removal of Heavy Metals from Aqueous Solution, *Bioresour. Technol.*, **320**: 124278 (2021).

[42] Sohaimi K.S.A., Ngadi N., Mat H., et al., Synthesis, Characterization and Application of Textile Sludge Biochars for Oil Removal, *J. Environ. Chem. Eng.*, **5**: 1415–1422 (2017).

[43] Nanda S., Mohanty P., Pant K.K., Characterization of North American Lignocellulosic Biomass and Biochar's in Characterization of North American Lignocellulosic Biomass and Biochar's in Terms of their Candidacy for Alternate Renewable Fuels, *Bioenergy Resour.*, **6**: 663–676 (2013).

[44] Behazin E., Ogunsona E., Rodriguez-Uribe A., et al., Mechanical, Chemical, and Physical Properties of Wood and Perennial Grass Biochars for Possible Composite Application, *Bio. Resources*, **11**: 1334–1348 (2016).

[45] Chow L.W., Tio S.A., Teoh J.Y., et al., Sludge as a Relinquishing Catalyst in Co-Pyrolysis with Palm Empty Fruit Bunch Fiber, *J. Anal Appl. Pyrolysis*, **132**: 56–64 (2018).

[46] Liang H., Chen L., Liu G., Zheng H., Surface Morphology Properties of Biochar's Produced from Different Feedstocks. In: International Conference on Civil, *Transportation and Environment*, 1205–1208 (2016).

[47] Giorcelli M., Khan A., Pugno NM., et al., Biochar as Cheap and Environmental Friendly Filler Able to Improve Polymer Mechanical Properties, *Biomass and Bioenergy*, **120**: 219–223 (2019).

[48] Lateef A., Nazir R., Jamil N., et al., Synthesis and Characterization of Environmental Friendly Corncob Biochar Based Nano-Composite – A Potential Slow Release Nano-Fertilizer for Sustainable Agriculture. Environ Nanotechnology, *Monit Manag*, **11**: 100212 (2019).

[49] Jeon J., Park J.H., Wi S., et al., Characterization of Bio Composite Using Coconut Oil Impregnated Biochar as Latent Heat Storage Insulation, *Chemosphere*, **236**: 124269 (2019).

[50] Boumanchar I., Chhiti Y., M'hamdiAlaoui F.E., et al., Effect of Materials Mixture on the Higher Heating Value: Case of Biomass, Biochar and Municipal Solid Waste, *Waste Manag.*, **61**: 78–86 (2017).

[51] Palodkar A.V., Anupam K., Banerjee S., Haldera G., Insight into Preparation of Activated Carbon Towards Defluoridation of Waste Water: Optimization, Kinetics, *Equilibrium, and Cost Estimation. Environ Prog. Sustain Energy*, **36**: 1597–1611 (2017).

[52] Chen T., Zhang Y., Wang H., et al., Influence of Pyrolysis Temperature on Characteristics and Heavy Metal Adsorptive Performance of Biochar Derived from Municipal Sewage Sludge, *Bio. Resource Technol*., **164**: 47–54 (2014).

[53] Ding Y., Liu Y., Liu S., et al., Potential Benefits of Biochar in Agricultural Soils: A Review, *Pedosphere*, **27**: 645–661 (2017).

[54] Domingues R.R., Trugilho P.F., Silva C.A., et al., Properties of Biochar Derived from Wood and High-Nutrient Biomasses with the Aim of Agronomic and Environmental Benefits, *PLoS One,* **12**: 1–19 (2017).

[55] Elaigwu S.E., Rocher V., Kyriakou G., Greenway G.M., Removal of Pb^{2+} and Cd^{2+} from Aqueous Solution Using Chars from Pyrolysis and Microwave-Assisted Hydrothermal Carbonization of Prosopisafricana Shell, *J. Ind. Eng. Chem.*, **20**: 3467–3473 (2014).

[56] Keiluweit M., Nico P.S., Johnson M.G., Kleber M., Dynamic Molecular Structure of Plant Biomass-derived Black Carbon(Biochar)- Supporting Information, *Environ. Sci. Technol.*, **44**: 1247–1253 (2010).

[57] Jarboe L.R., Wen Z., Choi D., Brown R.C., Hybrid Thermochemical Processing: Fermentation of Pyrolysis-Derived Bio-Oil, *Appl. Microbiol. Biotechnol*., **91**: 1519–1523 (2011).

[58] Uchimiya M., Wartelle L.H., Klasson K.T., et al., Influence of Pyrolysis Temperature on Biochar Property and Function as a Heavy Metal Sorbent in Soil, *J. Agric. Food Chem.*, **59**: 2501–2510 (2011).

[59] Yao Y., Gao B., Zhang M., et al., Effect of Biochar Amendment on Sorption and Leaching of Nitrate, Ammonium, and Phosphate in a Sandy Soil, *Chemosphere*, **89**: 1467–1471 (2012).

[60] Zama E.F., Zhu Y.-G., Reid B.J., Sun G.-X., The Role of Biochar Properties in Influencing the Sorption and Desorption of Pb (II), Cd (II) and as (III) in Aqueous Solution, *J. Clean. Prod.*, **148**: 127–136 (2017).

[61] Chen C., Yan X.., Xu Y, et al., Activated Petroleum Waste Sludge Biochar for Efficient Catalytic Ozonation of Refinery Wastewater, *Sci. Total. Environ.*, **651**: 2631–2640 (2019).

[62] Pariyar P., Kumari K., Jain M.K., Jadhao P.S., Evaluation of Change in Biochar Properties Derived from Different Feedstock and Pyrolysis Temperature for Environmental and Agricultural Application, *Sci. Total Environ.*, **713**: 136433 (2020).

[63] Wei J., Tu C., Yuan G., et al., Assessing the Effect of Pyrolysis Temperature on the Molecular Properties and Copper Sorption Capacity of a Halophyte Biochar, *Environ. Pollut.*, **251**: 56–65 (2019).

[64] Mian M.M., Liu G., Activation of Peroxymonosulfate by Chemically Modified Sludge Biochar for the Removal of Organic Pollutants: Understanding the Role of Active Sites and Mechanism, *Chem. Eng. J.*, **392**: 123681 (2020).

[65] Zhang Y., Xu X., Zhang P., et al., Pyrolysis-Temperature Depended Quinone and Carbonyl Groups as the Electron Accepting Sites in Barley Grass Derived Biochar, *Chemosphere*, **232**: 273–280 (2019).

[66] Yin Q., Liu M., Ren H., Biochar Produced from the Co-Pyrolysis of Sewage Sludge and Walnut Shell for Ammonium and Phosphate Adsorption from Water, *J. Environ. Manage.*, **249**: 109410 (2019).

[67] Calisto V., Ferreira C.I.A., Santos S.M., et al., Production of Adsorbents by Pyrolysis of Paper Mill Sludge and Application on the Removal of Citalopram from Water, *Bioresour. Technol.*, **166**: 335–344 (2014).

[68] Gai X., Wang H., Liu J., et al., Effects of Feedstock and Pyrolysis Temperature on Biochar Adsorption of Ammonium and Nitrate, *PLoS One,* **9**: e113888 (2014).

[69] Angın D., Şensöz S., Effect of Pyrolysis Temperature on Chemical and Surface Properties of Biochar of Rapeseed (Brassica napus L.), *Int. J. Phytoremediation*, **16**: 684–693 (2014).

[70] Elnour A.Y., Alghyamah A.A., Shaikh H.M., et al., Effect of Pyrolysis Temperature on Biochar Microstructural Evolution, Physicochemical Characteristics, and its Influence on Biochar/ Polypropylene Composites, *Appl. Sci.*, **9**: 1149 (2019).

[71] Yakout S.M., Daifullah A.E.H.M., El-Reefy S.A., Pore Structure Characterization of Chemically Modifiedbiochar Derived from Rice Straw, *Environ Engg. Manag. J.*, **14**: (2015).

[72] Hadi P.,To M.-H., Hui C.-W., Lin C.S.K., McKay G., Aqueous Mercury Adsorption by Activated Carbons, *Water Res.*, **73**: 37-55 (2015).

[73] Pillay K., Cukrowska E.M., Coville N.J., Improved Uptake of Mercury by Sulphur-Containing Carbon Nanotubes, *Microchem. J.*, **108**: 124-130 (2013).

[74] Lyu H., Xia S., Tang J., Zhang Y., Gao B., Shen B., Thiol-Modified Biochar Synthesized by a Facile Ball-Milling Method for Enhanced Sorption of Inorganic Hg^{2+} and Organic CH_3Hg^+, *J. Hazard. Mater*, **384**: 121357 (2020).

[75] H. Ali, Jawada, M Azlan, M Ishakb , M .Ahlam, Response Surface Methodology Approach for Optimization of Color Removal and COD Reduction of Methylene Blue Using Microwave-Induced NaOH Activated Carbon from Biomass Waste, *Desalination and Water Treatment J.*, **62**: 208-220 (2017).

[76] H Ali. Jawad, Abdul Hameed A. Saud, L, Wilson L.D. et al., High Surface Area and Mesoporous Activated Carbon from KOH Activated Dragon Dragon Fruits Peels for Methylene Blue Dye Adsorption, *Chinese Journal of Chemical Eng.*, **32**: 281-290 ( ).